Magnetoresistive micro-displacement sensor based on magnetorheological fluid

Xiaolin Li[1], Jiangtao Zhang[1], Luyan Shen[1], Liming Qing[1], Qiang Fu[1, 2], Youyi Sun[1*], Yaqing Liu[1]

1.Shanxi Province Key Laboratory of Functional Nanocomposites, North University of China, Taiyuan 030051, P.R. China.

2.School of Civil and Environmental Engineering, University of Technology Sydney, Ultimo NSW 2007, Australia.

Abstract: A novel magnetoresistance material based on magnetorheological fluid (MRF) was developed for applications in micro-displacement sensor. The MRF samples were fabricated by dispersing carbonyl iron particles (CIP) into a magnetic ion liquid (MIL) composed of 1-methylethyl ether-3-butylimidazole cation and $[Fe_2Cl_7]^-$ anions. The magnetoresistance characteristics were also systematically tested. It was found that the resistance value of MRF with a CIP content of 20 vol% decreased from 125 to 24.4KΩ when increasing the magnetic field from 0 to 0.2 T. A sensor device was developed to study the displacement sensing characteristics of MRF, and found that the sensor had a high sensitivity of 0.1 Ω/μm and a high resolution of 10.0 μm. The excellent performance can be attributed to the low modulus and good stability of the MIL matrix, allowing for easy change of the resistance by controlling the magnetic field or displacement. In summary, these unique characters make the present MRF a promising magnetoresistance material with potential applications in displacement sensor.

Keywords: Magnetorheological fluids, Magnetic ionic liquids, Magnetoresistance, Displacement sensor.

Responding author: Fax: 86-351-3559669

E-mail address: syyi@pku.edu.cn (YY Sun)

1. Introduction

Displacement sensors have been extensively applied in industry for measuring the position and movement of objects, as well as for measuring other physical quantities which can first be converted into movement such as pressure, acceleration, strain, etc. [1]. Depending on the application, the most commonly used displacement sensors in industry are optical/laser, capacitive, eddy-current and magnetoresistive sensors [1-2]. Among these sensors, the magnetoresistive sensors and related applications have attracted a growing interest in the displacement domain due to their advantages of relatively high sensitivity, high resolution, high bandwidth, low noise, low power consumption and small size. In addition, since the magnetic field is not sensitive to the presence of non-conductive pollutants such as oil, dirt, dust and steam, it can be used stably in harsh environments [3-4]. The structure and property of sensing materials play an important role in determining performance of sensors [2]. The sensing materials of magnetoresistive displacement sensor are mainly made of metal and ceramic films in practical industry [5]. However, these current sensing films show relatively low processability and poor performance (i.e. insufficient sensitivity, low resolution), and thereby cannot meet growing demand in the industrial and consumer sensing applications [5-7]. Therefore, it is still an ambitious challenge to develop a new magnetic sensing material for application in magnetoresistive displacement sensor.

Magnetorheological gel (MRG) or elastomer (MRE) is a new type of magnetic sensing materials, which has the advantages of easy fabrication and excellent magnetoresistance, and can be potentially used in magnetoresistive displacement sensors [8-11]. For example, it has been reported that the resistance value of MRG with a carbonyl iron (CIP) content of 70 wt% decreased from 7.56 to 2.44 MΩ when increasing the magnetic field from 0.1 to 1.0 T [8]. The MRE composed of silicone matrix and nickel particles showed a giant magnetoresistance (GMR) with a decrease by three orders of magnitude for a field of only 100 kAm^{-1} (1250Oe) [9]. A new MRE consisting of PDMS matrix and Fe_3O_4@Ag particles with low resistance (ca. 1~10Ω) was prepared and its conductivity was improved by 50% under a magnetic field of 400 mT [10]. A new MRE composed of silicon matrix, graphite and carbonyl iron powders was developed and its conductivity was improved by three orders of magnitude under a 20 mT magnetic field [11]. These studies have indicated the excellent magnetoresistance performance of these MREs (and/or MRGs), which was

attributed to the magnetically induced strain of matrix and/or the magnetically induced alignment of magnetic particles [8-11]. However, there are few reports of MREs (or MRGs) used in magnetoresistive displacement sensors [8-11]. This is because these MREs (or MRGs) have relatively high modules and viscoelasticity, which restricts their magnetically-induced deformation and magnetically-indued motion of magnetic particles, resulting in low resolution, low bandwidth and large hysteresis [12]. Compared with MREs (or MRGs), the MRFs usually displayed lower modulus or viscosity, and thereby the magnetic particles in the matrix showed smaller viscous resistance and faster response under the same magnetic field [13]. However, traditional water-based or silicone oil-based MRFs showed poor anti-sedimentation stability, restricting their practical applications in sensors [14-15]. In addition, up to now, there is no report on MRF-based magnetoresistive displacement sensors.

To overcome above challenges, a new magnetic ionic liquid (MIL) composed of 1-methylethyl ether-3-butylimidazole (MBM) cation and $[FeCl_4]^-$ anion was synthesized. Then, the MIL was used as a new carrier of MRF for application in magnetoresistive displacement sensors. The cation of MIL can effectively improve anti-sedimentation stability of the resultant MRF, while the $[FeCl_4]^-$ anion and the CIP can effectively enhance the conductivity and magnetic response of MRF. In addition, the resulting MIL exhibited a low modulus or viscosity, thus the magnetic particles in matrix can move quickly and be easily aligned in the direction of the magnetic field, resulting in excellent magnetoresistive performance. These characteristics make the MIL-based MRF a promising magnetic sensing material for displacement sensors. In this study, firstly, the chemical structure and magnetic properties of MIL is characterized. Secondly, the principle of magnetoresistive displacement sensor is investigated. Then, the sensitivity, resolution, and stability for the magnetoresistance of magnetoresistive sensor based on MRF were systematically discussed and analyzed. Finally, we studied the feasibility of using the displacement sensor for bridge expansion joint monitoring.

2. Experimental

2.1 Material

1-Butylimidazole (>98%)，1-Chlorobutane (>98%) and the $FeCl_3 \cdot 6H_2O$ (>99%) were used to synthesize MIL. The carbonyl iron fibers (>97.7%) with a density (7.63g cm^{-3}) have a mean particle size of 0.1~0.4μm. The dichloromethane (AR >99.9%),

Chloromethyl ether (CP, >95%), Deuterated dimethyl sulfoxide (DMSO-d6 >99.9%) and ethyl acetate (AR, >99%) were purchased from the chemical market. All other chemicals (analytical grade) were obtained commercially and used without further purification unless otherwise stated.

2.2 Preparation of MRF based on MIL

The MIL was synthesized by a two-step method as shown in following. Firstly, 16.2 g 1-butyl imidazole and 10.0 g chloromethyl ether were dissolved in 20 mL dichloromethane under stirring at 9 ^{o}C. The suspension was reacted at 30 ^{o}C for 3 h under the protection of N_2. The products were washed with dichloromethane and ethyl acetate twice, forming pure ionic liquids. Secondly, 39.6 g $FeCl_3 \cdot 6H_2O$ was added to above ionic liquid (ca.16.0g) under vigorous stirring and further reacted at 30 ^{o}C for 3 h under the protection of N_2. Finally, the products were purified by rotary evaporator and dried in a vacuum oven at 60 ^{o}C for 24 h, forming MIL.

MRF (5-20 vol%) were prepared by combination of CIPs and MIL. Firstly, the CIPs were dispersed in acetone at room temperature under ultrasonic treatment for 1 h. Then the MIL was added to above mixture under ultrasonic treatment for another 1 h. Finally, the suspension was maintained at 80 ^{o}C for 4 h to remove the acetone, forming MRF based on MIL.

2.3 Characterizations

The resultant and intermediate products were characterized by ^{1}H-NMR on a Avance III 600MHz NMR spectrometer at room temperature, using dimethyl sulfoxide-d6 (DMSO-d_6) as solvent.

Infrared spectroscopy (FT-IR) spectra were performed on a Thermo Fisher Spectrum One (Thermo Fisher, USA) and scanned from 500 to 4000 cm^{-1}.

Raman measurement was carried out by In Via at a wavelength of 785 nm at 298 K.

The magnetic properties of carbonyl iron fiber and MILs were measured at room temperature by vibrating sample magnetometer (MicroSense, LLC, USA) from -11000 Oe to 11000 Oe.

Anti-sedimentation stability of MILs was measured as shown in following. The MRF was transferred in the cylindrical polyethylene tube with a diameter and length of 1.2 mm×5.0 mm. Approximately 2.5 mL MRF was left to settle at rest at room temperature. For a period, a supernatant layer appeared because of the gravity-induced sedimentation of magnetic particle. The sedimentation ratio was

obtained according to the following equation 1[16]:

Sedimentation ratio (%) $=H/H_0\times100$ (1)

The H_0 (mm) and H (mm) are the initial height of the suspension in the tube and height of the supernatant layer as function of time, respectively.

Magnetoresistive performance of MRF was characterized as shown in following. The test sample was obtained by injecting MRF into the soft plastic tubes and then encapsulating it. Firstly, the prepared MRF with a carbonyl iron content of 5~20vol% was injected into hoses through a needle tube, in which the outer and inner diameter of hose with a length of 80 mm was 3.6 mm and 3.0 mm, respectively. Secondly, the coiled conductive copper wire is embedded into both ends of the hose. Finally, epoxy adhesive was used to end-capping, avoiding leakage during the tests.

The magnetoresistance of MRF was determined as function of magnetic fields by a self-assembled magnetic field generator and a DC Resistance Meter (Tong hui, TH2516B) as shown in Fig.1. The tested sample was fastened to the center of the solenoid coil. The magnetic field strength was controlled through the current controller. The external magnetic field was applied for 6 seconds and then removed. At the same time, high-speed camera was used to record the resistance change of sensor as function of magnetic field strength (0~1.0T).

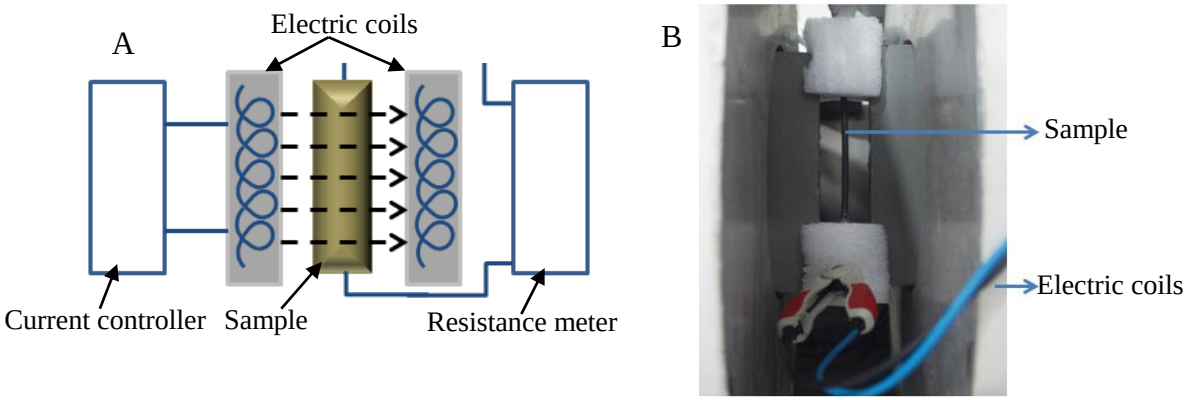

Fig.1. (A)Schematic diagram and (B) Optical photo of magnetoresistance test.

2.4 Characteristics of displacement sensor based on MRF

The displacement sensor was mainly composed of soft plastic tubes containing with MRFs, permanent magnet and DC Resistance Meter as shown in Fig.2. When the displacement sensor parallelly moves away from the magnet in the direction (0.0-5.0cm) as shown in Fig.2A, the resistance of soft plastic tubes continuously changes. According to the relationship between moving displacement and resistance,

the moving displacement was determined by the measured resistance. In order to verify accuracy of displacement, vernier caliper was further used to measure the displacement. The sensitivity (S, Ω/μm) and measuring error (ME, %) of senor is obtained using the following formula:

$$S = \frac{R_d - R_0}{d} \text{ and } ME = \frac{D1 - D2}{D1}$$

Where, R_0 and R_d are the resistance values before and after movement, respectively. d is the moving displacement. $D1$ and $D2$ are the moving displacement by present sensor and vernier caliper, respectively. Here, the resolution is defined as the smallest detectable displacement, in which a smallest change in resistance can be observed in DC Resistance Meter under moving displacement.

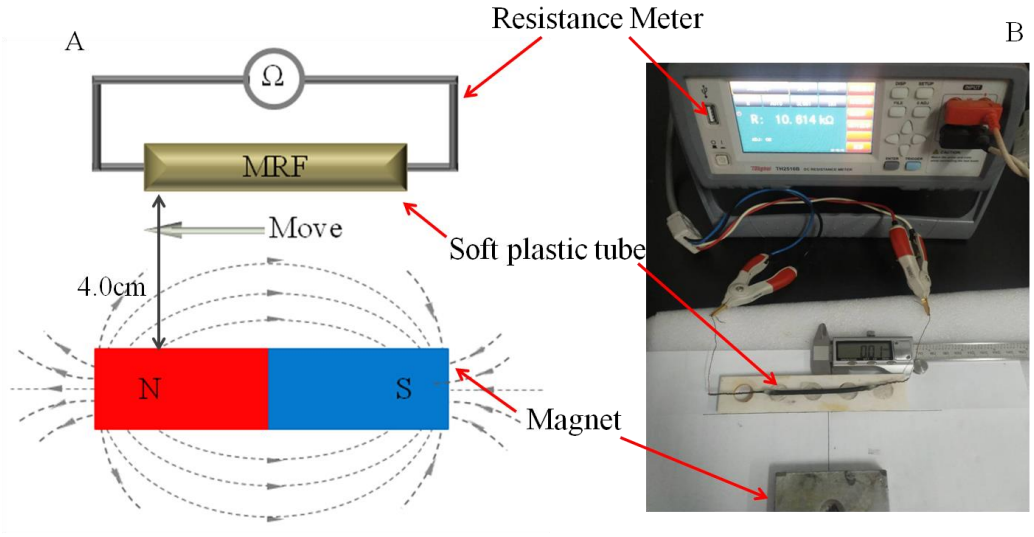

Fig.2. (A)Working principal diagram and (B)Optical photograph of displacement sensor device.

3. Results and discussion

3.1 Synthesis and characterization of MIL

The successful preparation of MIL was firstly confirmed by the ^{1}H-NMR spectrum as shown in Fig.3A and the data are listed as follow: MIL, δ=9.47 (s, 1H, -N=C***H***-N-), 7.91 (s, 2H, -N-C***H***=C***H***-N-), 5.53 (s, 2H, CH_3-C***H***$_2$-O-), 4.73 (s, 2H, CH_3-C***H***$_2$-O-), 4.23 (s, 2H, -N-C***H***$_2$-CH_2-), 1.81 (t, 2H, J=3.6Hz, -CH_2-C***H***$_2$-CH), 1.28 (s, 2H, -C***H***$_2$-CH_3), 0.92 (s, 6H, -C***H***$_3$). The Raman spectrum of MIL was also characterized as shown in Fig.3B. A absorption peak at 420 cm^{-1} was clearly observed as shown in Fig.3B, which was assigned to $Fe_2Cl_7^-$[17]. The FT-IR spectrum of MIL

was further characterized as shown in Fig.3C. The wide absorption band around 3355 cm^{-1} was attributed to intermolecular hydrogen bonding [18]. The absorption peaks around 3149~2954 cm^{-1} were assigned to C-H stretching modes of the imidazolium ring [19]. The absorption peaks around 1604.0cm^{-1} and 1557.0cm^{-1} were assigned to C=C stretching vibrations on the imidazolium ring [18]. The absorption peaks at 1157 cm^{-1} and 1108~1104 cm^{-1} were assigned to C-N stretching modes and C-O stretching modes, respectively [18, 20]. The absorption peaks below 1000 cm^{-1} were assigned to C-C or C-N bending vibration [20]. These results indicated the successful synthesis of MIL. The magnetic property of MIL was characterized by Vibrating Sample Magnetometer (VSM) method magnetization and magnetic field strength in magnetic field range of -11000 to 11000 Oe at 298K as shown in Fig.3D. It clearly showed linear response to the magnetic field, indicating a paramagnetic performance [21]. The permeability of MIL was determined to be 1.768×10^{-5}. The result indicated the successful preparation of MIL with magnetic property.

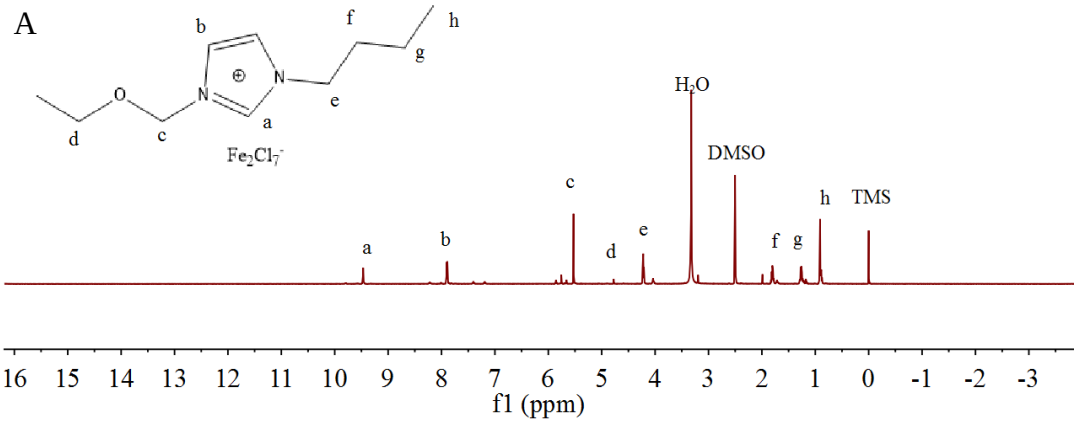

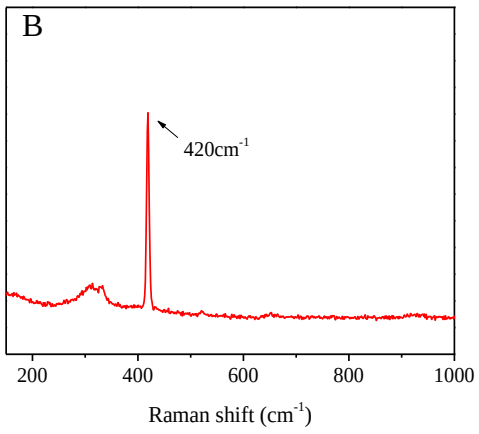

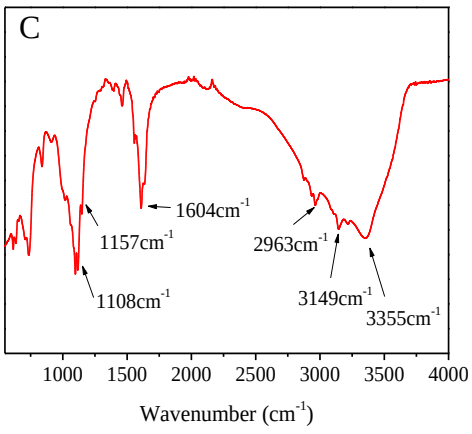

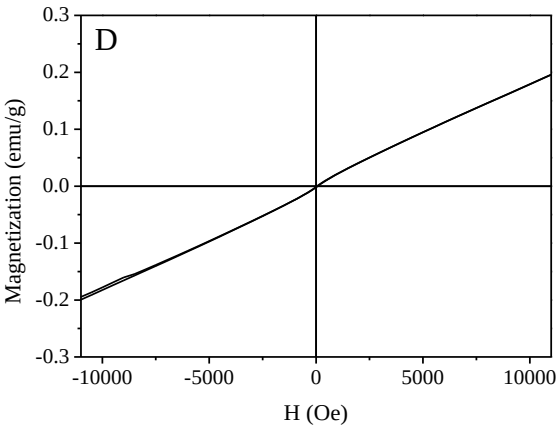

Fig.3. (A) 1H-NMR, (B) Raman spectra and (C) FT-IR of MIL, and (D) Magnetic curve of MIL as functions of magnetic field at 298 K.

3.2 Magnetoresistive performance of MRF based on MIL

Although the magnetorheological properties of MRFs have been reported, yet their magnetoresistive properties were few reported. Here, magnetoresistive properties of MRF composed of MIL and CIP were investigated in detail as a function of CIPs content as shown in Fig.4A. The resistance of MRFs linearly decreased with increasing in magnetic field strength to 300 mT. The resistance sharply dropped from 290 KΩ, 230 KΩ, 183 KΩ, 121 KΩ to 177 KΩ, 128 KΩ, 62 KΩ, 18 KΩ for the MRFs with 5, 10, 15 and 20 vol% CIP loads, respectively. The magnetic sensitivity of present MRFs was calculated to be 0.1Ω/μm. This result demonstrated that the present MRF had potential applications in micro-displacement sensor. When the magnetic field strength was further improved, yet the resistance was slightly changed. The result was attributed to magnetorheological effect of MFRs as shown in Fig.4B. Under low magnetic field strength (0~300mT), the CIPs gradually polarized and formed magnetic chains from the state of being freely dispersed in the matrix [22], resulting in a sharp drop of resistance. When the magnetic field strength was further improved to more than 300 mT, the magnetic chains changed slightly, resulting in a slight change in resistance. These results indicated that present MRFs based on MIL and CIPs possessed good magnetoresistive properties. Moreover, the magnetoresistance of present MRF maintains a good linear relationship between resistance and magnetic field strength under low magnetic field (<250 mT) [8-11], especially for MRF with a CIP load of 20 vol%. This linear characteristic of MRF is the key to its application in magnetoresistive displacement sensor. Magnetoresistance hysteresis of MRFs was also characterized under the magnetic field of 0.3-0.45T as shown in Fig.4C. It was found that the resistance of MRF rapidly decreased and then

reached a steady-state value within 1.5s. When the magnetic field was turned off after 6s, the resistance value could be quickly restored within 1.5s. Interestingly, no magnetoresistive hysteresis was observed. These results indicated that present MRF had a fast response and recoverable performance toward magnetic field. In a comparison, the traditional MRGs usually had a large hysteresis and a slow response time of *ca.* 9s [8]. The different result is attributed to that these magnetic particles can be quickly magnetized, attracted each other along the magnetic field lines in MIL (in Fig.4B), leading to a fast increase of resistance [22]. When the magnetic field is removed, these aligned magnetic particles are recover to random distribution in MIL with low viscosity [22].

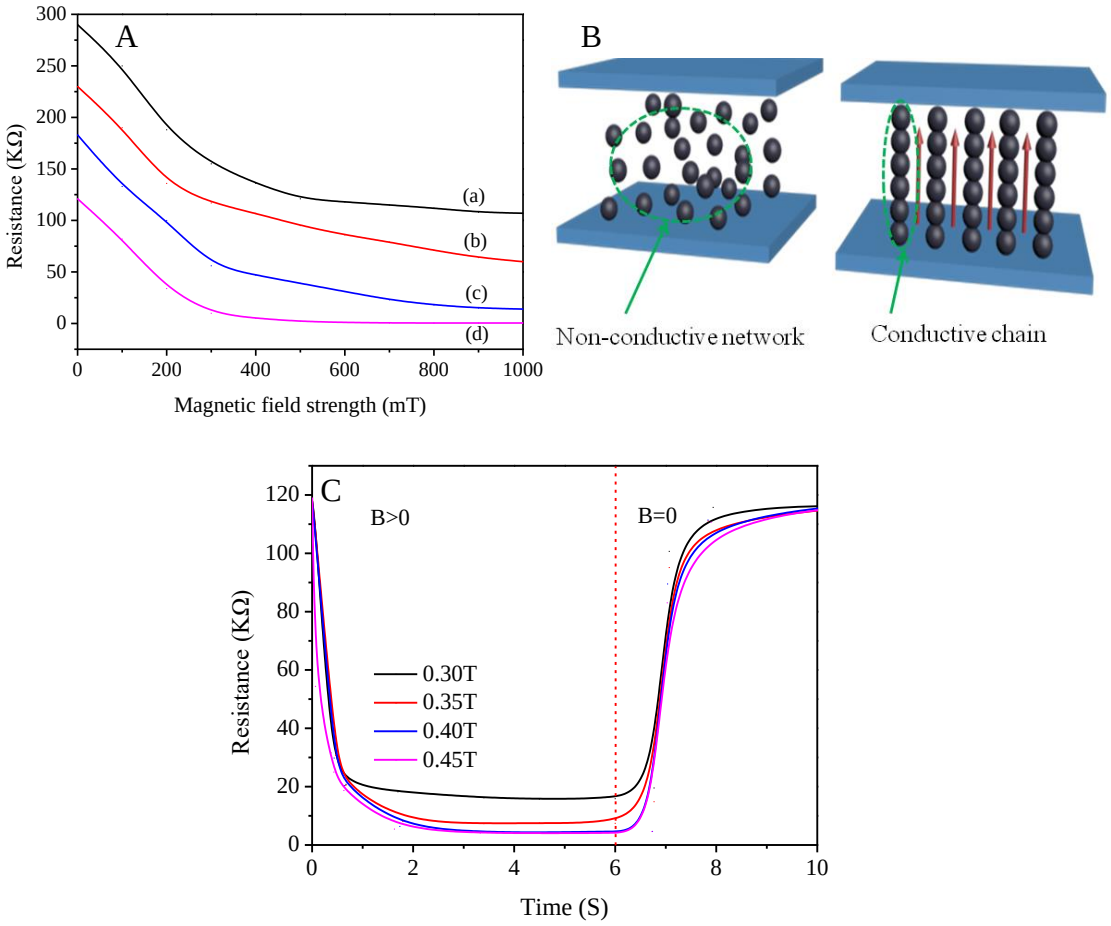

Fig.4. (A) Magnetoresistance curve of MRFs with CIPs loads of (a) 5, (b) 10, (c) 15 and (d) 20 vol%., (B) Magnetoresistive mechanism of present MRF, (C) Magnetoresistive hysteresis of the displacement sensor was tested under various magnetic fields of 0.3, 0.35, 0.4 and 0.45T.

3.3 Performance of displacement sensor based on MRF

As well-known, the magnetic field strength was also controlled by adjusting the distance to magnet. As shown in Fig.5A, the magnetic field strength linearly

decreased with increasing in the distance from 0 to 3.25 cm. So, the displacement sensor was designed and fabricated by assembling sensing materials based on MRF, magnet and DC Resistance Meter as shown in Fig.2. The relationship between displacement and the resistance of displacement sensor were characterized as shown in Fig.5B. The resistance obviously increased with the increase of displacement, and there was a good linear correlation between them within 3.25 cm. We then derived the derivation of the horizontal displacement-resistance relationship curve and found that the d_R/d_X was a constant within 3.25 cm. This result further confirmed that present sensor based on MRFs showed a good linear response within a certain displacement range (3.25 cm). The linear relationship between displacement and resistance can be fitted as following equation: $R(\Omega)=0.10147(\Omega/\mu m)\bullet x+10624$. The measuring and theoretical resistance (calculated by above equation) of the displacement sensor after a slight movement in the horizontal direction are listed in Table 1. Here, the smallest displacement and resistance that can be identified/detected under the current test condition are 10 μm and 0.001 KΩ, respectively. This result indicates that the present displacement sensor has a resolution of 10 μm, and if a current controller with higher resolution is used, this value can be further improved. The calculated measurement Error is about 1.4%, which further demonstrates the accurate detection capability of the prepared displacement sensor. In contrast, conventional MREs commonly showed a nonlinear response to distance, restricting their applications in displacement sensor [23].

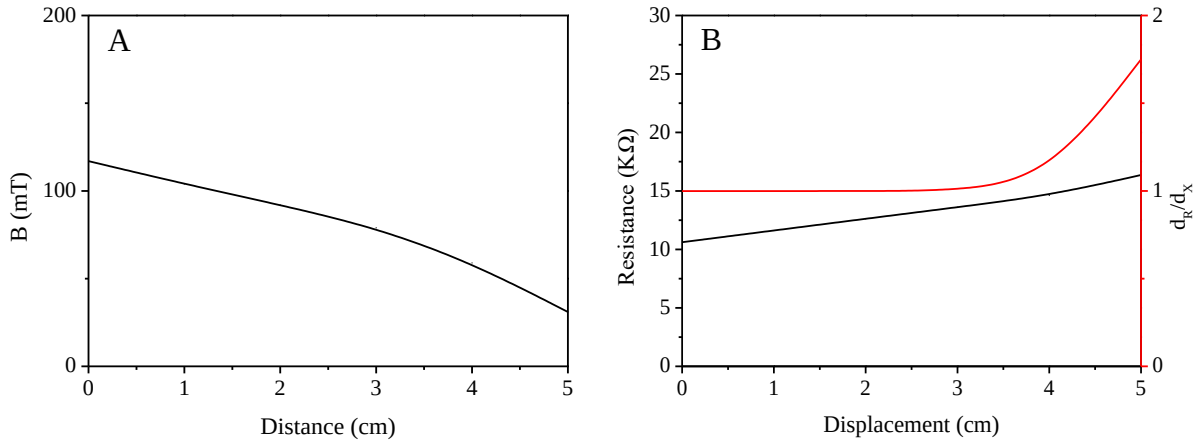

Fig.5. (A) Magnetic field strength of magnet as function of moving displacement. (B) Resistance-displacement curve and magnetic sensitivity of the MRF-displacement sensor. Of particular note, the displacement refers to the relative distance between the center axis of the permanent magnet and the sensor in the horizontal direction.

Table 1. The measuring resistance and theoretical resistance of the MRF-displacement sensor after a slight movement in the x direction. (0.1Ω/μm).

Measuring resistance(KΩ)	Measuring Displacement(μm)	Theoretical Displacement(μm)	Error %
10.624	0	0	0
10.625	10	9.86	1.40
10.626	20	19.71	1.45
10.627	30	29.57	1.43
10.628	40	39.42	1.45
10.629	50	49.28	1.44

The stability of displacement sensors based on MRF was further evaluated as shown in Fig.6A. It clearly showed that all resistance-displacement curves measured on 0, 5, 10, 20, and 30 days were identical, indicating that the displacement sensor had good stability for long-term use. The good stability was attributed to the good anti-sedimentation of MRF. As shown in Fig.6B, the sedimentation ratio of the present MRF after 3 months was *ca.* 7.4%, which was lower than that of conventional MRFs (*ca.* 20%) reported in previous work [25]. The result demonstrates that the present MRF has good anti-sedimentation performance, which was attributed to the special structure of MIL. As shown in Fig.6C, the $[Fe_2Cl_7]^-$ anions easily formed a network structure, meanwhile the anions with large steric hindrance could prevent the formation of ion pairs, thereby promoting the interaction between magnetic particles and cations. These effects together limited the sedimentation of magnetic particles. To further illustrate the application performance of the magnetoresistive displacement sensor based on MRF [26-29], we compared the performance of five typical displacement sensors based on other sensing materials and the results were listed in Table 2. It was found that the present displacement sensor had better overall performance than other sensors, including relatively large measurement range, high resolution, high sensitivity, low-cost and simple setup. Although the experimental results obtained have a relatively high systematic error due to the inherent accuracy limitation of the instrument, but if the hardware is improved, this shortcoming can be overcome. Therefore, the present displacement sensor has great potential in real industrial applications.

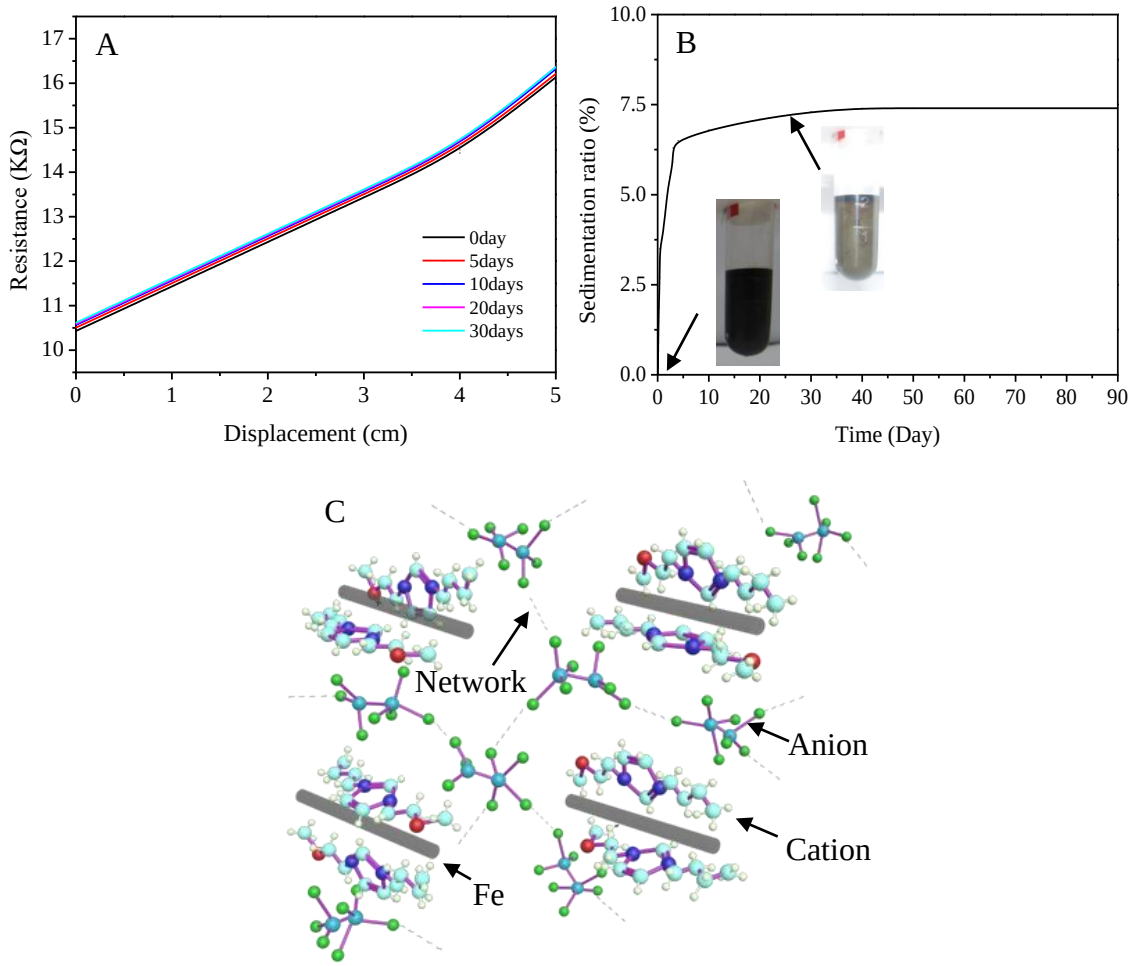

Fig.6. (A) The resistance-displacement curve of the MRF-displacement sensor as function of holding days, (B) Sedimentation ratio of MRF with CIPs content of 20.0vol% as function of holding time, (C) Micro-structure and stable mechanism of MRF. The inset of B is the optical photographs of MRFs based on MIL at holding time of 0 and 30 days.

Table 2. Comparison of other typical displacement sensors and magnetoresistive displacement sensor based on other materials.

Principle	Measurement Range (mm)	Resolution (μm)	Sensitivity	Error %	Cost	Complexity	Reference
Magnetore sistive	40	10	0.1Ω/μm	1.44	Low	simple	present
	0.04	0.033	17.0 mV /μm	------	Low	moderate	[24]
	14	------	12μmV/μm	------	Low	moderate	[6]
Capacitive	40	18	1.36 pF/mm	0.6	Low	moderate	[26]
Laster	11.8	0.0149	60.4mV/μm	0.9	High	complex	[27]
Eddy	140	2.67	------	1.0	Low	complex	[28]

As well-known, wind, temperature, vehicle load and other factors may cause the vertical displacement of the expansion joint on the bridge (Fig. 7) [30]. Once the expansion joint gap is too large, it will have various adverse effects on the bridge [31]. In this study, we also used the present displacement sensor to check the working performance of the bridge expansion joints in time. The bridge expansion joint model was prepared by the 3D printer shown in Fig.7. When part-B of the bridge expansion joint slides horizontally along the slide rail, the movement displacement is measured in real time according to the resistance value. It was found that the observed results were highly consistent with the measured values of vernier caliper (Table 3). This result again proves that the present micro-displacement sensor has high-precision displacement measurement and can be used in practical applications.

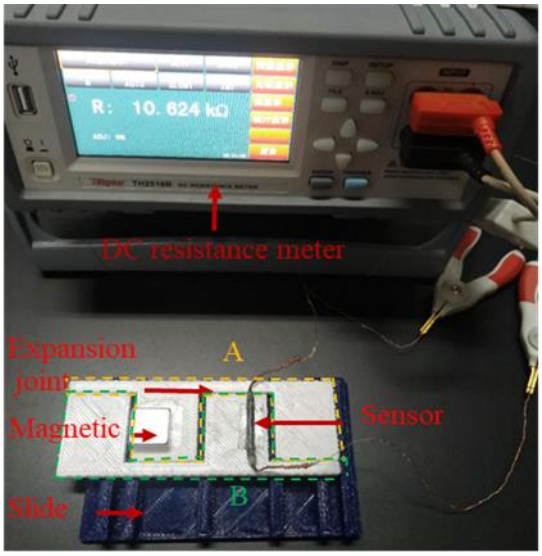

Fig.7. Bridge expansion joint prototype and displacement sensor installation model.

Table.3 Comparison of displacement of bridge expansion joints measured by sensor and vernier caliper.

Measured by sensor (μm)	Measured by vernier caliper (μm)	Error (%)
98.56	100	1.44
197.16	200	1.42
295.71	300	1.43
394.36	400	1.41
492.95	500	1.41

4.Conclusion

In this work, a new MIL-based magnetorheological fluid (MRF) was synthesized

and developed. Furthermore, its magnetic and displacement sensing performance were also studied by assembling a magnetoresistive micro-displacement sensor. It is found that the prepared displacement sensor has high sensitivity (0.1Ω/μm), high resolution (10μm) and high-precision displacement measurement. This study therefore opens a new avenue for the development of displacement sensors for real-time measurement in various industrial applications.

Acknowledgements

The authors are grateful for the support of the National Natural Science Foundation of China under grants (51773184 and U1810114), and Shanxi Provincial Natural Science Foundation of China (201701D121046 and 201803D421081).

References

[1] S.K. R, B. George, J.K. V, Combined Variable Reluctance-Hall Effect Displacement Sensor, IEEE Transactions on Instrumentation & Measurement, 2017,67,1-9.

[2] O. Kypris, A. Markham, 3-D Displacement Measurement for Structural Health Monitoring Using Low-Frequency Magnetic Fields, IEEE Sensors Journal, 2017,17,322-224.

[3] B. George, Z. Tan, S. Nihtianov, Advances in Capacitive, Eddy Current and Magnetic Displacement Sensors and Corresponding Interfaces, IEEE Transactions on Industrial Electronics, 2017,64,1-1.

[4] V. Kartik, A. Sebastian, T. Tuma, A. Pantazi, H. Pozidis, D.R. Sahoo, High-bandwidth nanopositioner with magnetoresistance based position sensing, Mechatronics, 2012,22, 295-301.

[5] P. Ripka, M. Janosek, Advances in Magnetic Field Sensors, IEEE Sensors Journal, 2010,10,1108-1116.

[6] B. Kaviraj, S.K. Ghatak, Magnetic Field and Displacement Sensor Based on Giant Magneto-Impedance Effect, Materials and Manufacturing Processes, 2006, 21,271-274.

[7] P.S.S. Parkin, Giant Magnetoresistance in Magnetic Nanostructures, Annual Review of Materials Research, 1995,25,357-388.

[8] M. Yu, B. Ju, J. Fu, S. Liu, S.-B. Choi, Magnetoresistance Characteristics of Magnetorheological Gel under a Magnetic Field, Industrial & Engineering Chemistry Research , 2014, 53,4704-4710.

[9] N. Kchit, P. Lancon, G. Bossis, Thermoresistance and giant magnetoresistance of

magnetorheological elastomers, Journal of Physics D: Applied Physics, 2009,42,105506.

[10] J.L. Mietta, M.M. Ruiz, P.S. Antonel, O.E. Perez, A. Butera, G. Jorge, R.M. Negri, Anisotropic magnetoresistance and piezoresistivity in structured Fe3O4-silver particles in PDMS elastomers at room temperature, Langmuir : the ACS journal of surfaces and colloids, 2012,28 6985-96.

[11] X.G. Huang, Z.Y. Yan, C. Liu, G.H. Li, J. Wang, Study on the resistance properties of magnetorheological elastomer, Materials Research Innovations , 2015,19,S5-924-S5-928.

[12] N.H.N.A. Hadi, H. Ismail, M.K. Abdullah , Influence of matrix viscosity on the dynamic mechanical performance of magnetorheological elastomers, Journal of Applied Polymer science, 2019,137,48492.

[13] Z.-D. Xu, W.-Y. Guo, B.-B. Chen, Preparation, Property Tests, and Limited Chain Model of Magnetorheological Fluid, Journal of Materials in Civil Engineering, 2015,27, 04014229.

[14] D. Bica, L. Vékás, M.V. Avdeev, O. Marinică, V. Socoliuc, M. Bălăsoiu, V.M. Garamus, Sterically stabilized water based magnetic fluids: Synthesis, structure and properties, Journal of Magnetism and Magnetic Materials,2007, 311,17-21.

[15] X. Liu, H. Lu, Q. Chen, D. Wang, X. Zhen, Study on the Preparation and Properties of Silicone Oil-Based Magnetorheological Fluids, Materials and Manufacturing Processes, 2013, 28,631-636.

[16] H.B. Cheng, J.M. Wang, Q.J. Zhang, N.M. Wereley, Preparation of composite magnetic particles and aqueous magnetorheological fluids, Smart Materials and Structures, 2009,18, 085009.

[17] T. Bäcker, O. Breunig, M. Valldor, K. Merz, V. Vasylyeva, A.-V. Mudring, In-Situ Crystal Growth and Properties of the Magnetic Ionic Liquid [C2mim][FeCl4], Crystal Growth & Design, 2011,11 2564-2571.

[18] C. Chen, A functionalised ionic liquid: 1-(3-chloro-2-hydroxypropyl)-3-methyl imidazolium chloride, Physics and Chemistry of Liquids, 2010,48, 298-306.

[19] L. Tao, J. Lu, B. Hu, J. Chen, S. Xu, F. Liu, D. He, Synthesis and characterisation of new polymeric ionic liquid poly(imidazolium chloride-4,6-dinitrobenzene-1,3-diyl), Materials Research Innovations, 2014,19, 65-68.

[20] B. Haddad, D. Mokhtar, M. Goussem, E.-h. Belarbi, D. Villemin, S. Bresson, M.

Rahmouni, N.R. Dhumal, H.J. Kim, J. Kiefer, Influence of methyl and propyl groups on the vibrational spectra of two imidazolium ionic liquids and their non-ionic precursors, Journal of Molecular Structure, 2017, 1134, 582-590.

[21] G. Wang, F. Zhou, Z. Lu, Y. Ma, X. Li, Y. Tong, X. Dong, Controlled synthesis of CoFe2O4/MoS2 nanocomposites with excellent sedimentation stability for magnetorheological fluid, Journal of Industrial and Engineering Chemistry, 2019, 70,439-446.

[22] X. Chen, X. Zhu, Z. Xu, Y. Lin, G. He, The research of the conductive mechanism and properties of magnetorheological fluids, Physica B: Condensed Matter, 2013, 418 , 32-35.

[23] G. Ausanio, V. Iannotti, E. Ricciardi, L. Lanotte, L. Lanotte, Magneto-piezoresistance in Magnetorheological elastomers for magnetic induction gradient or position sensors, Sensors and Actuators A: Physical, 2014,205,235-239.

[24] L. Liu, Y. Yang, B. Yang, Non-contact and high-precision displacement measurement based on tunnel magnetoresistance, Measurement Science and Technology, 2020,31, 065102.

[25] A.J.F. Bombard, F.R. Gonçalves, J. Vicente, Magnetorheology of Carbonyl Iron Dispersions in 1-Alkyl-3-methylimidazolium Ionic Liquids, Industrial & Engineering Chemistry Research, 2015, 54, 9956-9963.

[26] N. Anandan, B. George, A Wide-Range Capacitive Sensor for Linear and Angular Displacement Measurement, IEEE Transactions on Industrial Electronics, 2017,64,1-1.

[27] C. Prelle, F. Lamarque, P. Revel, Reflective optical sensor for long-range and high-resolution displacements, Sensors and Actuators A: Physical, 2006, 127, 139-146.

[28] L. Wu , Q. Tang, X. Chen , A Novel Two-Dimensional Sensor With Inductive Spiral Coils, IEEE Sensors Journal, 2019,19,1-1.

[29] S.K. R, B. George, J.K. V,Combined Variable Reluctance-Hall Effect Displacement Sensor, IEEE Transactions on Instrumentation & Measurement, 2017,67,1-9.

[30] L.M. Chang, Y.J. Lee, Evaluation of Performance of Bridge Deck Expansion Joints, Journal of Performance of Constructed Facilities, 2002, 16, 3-9.

[31] Y. Ding, A. Li, Assessment of bridge expansion joints using long-term displacement measurement under changing environmental conditions, Frontiers of

Architecture&Civil Engineering, 2011, 5, 374-380.